The Proceedings of the 10th International Symposium on Computer Methods in Biomechanics and Biomedical Engineering. Hotel Berlin, Berlin, Germany, April 7th – 11th, 2012. Published by ARUP; ISBN: 978-0-9562121-5-3; Available in www.cmbbe2012.cf.ac.uk

Preface:
The 10th International Symposium on Computer Methods in Biomechanics and Biomedical Engineering was held in Berlin, Germany in April 2012 and follows the meetings held in Swansea 1992/94, Barcelona 1997, Lisbon 1999, Rome 2001, Madrid 2004, Antibes 2006, Porto 2008 and Valencia 2010. This tenth symposia of the series was developed through the direct input of an international cohort of some thirty invited speakers and special session chairs and hence provided a programme of innovative research, new and novel techniques and the latest developments taking place in the field of computational biomechanics and bioengineering.

Developments in this multidisciplinary area continue unabated and many of presentations extended, advanced and introduced new topics including cellular and biomolecular mechanics, multi scale modelling including local-global cell/biological dynamics and neural/brain IT. Contributions on spine/knee and musculosketal biomechanics were also well represented as were bioimaging and visualisation techniques which encompass areas including patient response to biomarkers and nanoparticle targeted systems as well as the identification of the mechanical properties of biological materials and tissue structure. Advances in hemodynamics and the virtual physiological human were also presented and the symposium was further enhanced with plenary talks from world leading medical device organisations who now consider computational biomechanics as an indispensable tool in new product development.

Computational biomechanics is now an accepted platform for simulating the behaviour, processes and outcomes of complex tissue structures and is widely used in research laboratories, commercial establishments and the medical technology sector as well as being an increasingly powerful tool within the clinical environment. Advances in imaging/visualisation and data capture now provide both an accurate and cost effective means of studying tissue structure and function and software systems are being increasingly used as a test bed to predict cell interaction, drug targeting and tissue regeneration. Here multiscale modelling can provide a unique opportunity to correlate what a biologist sees in a dish to what a clinician measures in the patient, also data on cellular forces, mechanical properties and mechanical function of cells and organelles, will ultimately provide a better understanding of how cells actually function and how they react to their environment. Many of the research groups present at the symposium have now developed multidisciplinary groups with a high level of computational expertise together with strong biosciences and clinical input and it is considered that these groups hold a passport to the successful study of the complex nature of biological systems as well as the ability to improve and introduce new solutions within the healthcare sector.

As well as the many oral and poster presentations which formed the symposium proceedings mini-symposia were organised by SIMPLEWARE and SIMULIA a and special workshop session was presented by Jeff Weiss on the latest features of FeBio. The other sessions which form these proceedings are subdivided into the following themes:

SS1: Multiscale modeling of biological systems
Chairs: Ellen Kuhl and Chris Jacobs

SS2: Spine and intervertebral disc biomechanics
Chairs: Richard Hall and Philippe K. Zysset

SS3: The virtual physiological human — from imaging to computer-aided medical practice
Chairs: Marc Thiriet and Jos Vander Sloten

SS4: Zimmer special session on upper limb biomechanics
Chairs: Andrew Hopkins and Joern Seebeck

PARAMETER IDENTIFICATION IN FUNCTIONAL AXIS CALCULATION FOR THE HUMAN KNEE JOINT

I. Reichl[1] and W. Auzinger[2]

1. ABSTRACT

The interpretation of joint kinematics data in terms of displacements is a product of the type of movement, the measurement technique and the underlying model of the joint implemented in parameter optimization procedures.
Misaligned knee joint axes do not only lead to a misinterpretation of knee joint kinematics but, additionally, have a general impact on lower body kinematics. Therefore, several groups independently propose different methods for *a posteriori* replacing the empirical flexion axis (determined from the original gait protocol) by a functionally calculated axis. Among the three main different rotations of the knee joint, flexion is the most dominant motion. Thus, if not determined accurately, it significantly affects any kinematical calculation. On the other hand, the large angular flexion range facilitates the mathematical procedure of axis determination. The second rotation of importance is the internal/external rotation which is sometimes controlled by mathematical optimization techniques. Consecutively to the axis reorientation process, joint displacements are computed via conventional procedures where knee rotation axes and consequently ankle and hip description have been modified.
This contribution focuses on the evaluation of methods for the determination of rotation axes via parameter identification. It is the purpose to elaborate which of the available mathematical algorithms performs most robust and convenient in selected clinical settings. Quality parameters for the calculated flexion axis are proposed.

2. INTRODUCTION

Computer assisted surgery requires that the kinematic description of joints is as accurate and reproducible as possible. It is an aim to ensure the comparability between different groups and clinics. In order to attain this objective, well-defined mathematical procedures have been developed in order to define the reference axes in a uniform, observer independent way, reconstructing these axes from kinematical data. In practice, the relevant reference axes are obtained by a mathematical optimization process based on an appropriate kinematical model of the joint in question.

For the intact knee joint, a common description is the compound hinge joint (CHJ)

[1]University of Vienna, Centre for Sport Science and University Sports, Department for Biomechanics/Kinesiology and Applied Computer Science, AT-1150 Vienna, Austria (e-mail: Irene.Reichl@univie.ac.at).
[2]Vienna University of Technology, Institute for Analysis and Scientific Computing, AT-1040 Vienna, Austria.

model. It approximates knee kinematics by a 2 DOF motion, including flexion and internal-external (ie) rotation. At first, a simple fitting procedure yields the main rotational axis, namely the flexion axis. Then the second axis is optimized. At the end, clinically determined axes may be replaced by these functionally calculated axes resulting in an improvement of the reproducibility of the observed 6 DOF displacement (Marin et al., 2003). However, there is no unique procedure for the accomplishment of these two steps. Churchill et al. (1998) determine the first axis from bony landmarks and optimize only the location of the second one. Martelli et al. (2002) and Marin et al. (2003) set the flexion axis equal to the calculated *finite helical axis* (FHA) (Woltring et al., 1987). However, alternative ways have been proposed in literature for the computation of a single rotational axis. Among these methods, the *symmetrical axis of rotation approach* (SARA) seems to perform best (Ehrig et al., 2007). It is the aim of this contribution to compare the performance of the SARA and the FHA approaches in the framework of the CHJ model.

3. MATERIAL AND METHODS

In the present study, the CHJ model is employed for the purpose of the kinematic data analysis. Here, the flexion axis is determined in two alternative ways, namely by means of the SARA or the FHA approach. For more details concerning the underlying methodology and numerical aspects of these implementations, see (Reichl and Auzinger, 2012).

3.1 Data

Kinematic data were generated by assuming a fictive knee joint. The data of Moglo and Shirazi-Adl (2005) constitute the basis for the simulated 6 DOF displacement between femur and tibia. The position of femur and tibia is tracked via four markers per segment. Soft tissue noise is modeled by trigonometric functions according to (Dumas and Chèze, 2009) where each marker has its individual frequency, amplitude and phase.

3.2 Data analysis

These fictive but typical data are analyzed with the aim to investigate which of the proposed computational algorithms performs best in recovering the original 6 DOF displacement. The calculation of the 6 DOF displacement is performed in three different ways utilizing alternative flexion axes. The first axis, usually unknown in an experimental setting, is introduced for test purposes and is identical to the flexion axis used to generate the fictive kinematic data. The second possible flexion axis is set equal to the axis calculated by means of the SARA. The third flexion axis is equal to the FHA.

Considering planar movement, namely pure flexion, both methods – SARA and FHA approach – yield the same flexion axis. Here, the movement can be regarded as 1 DOF displacement throughout the entire movement cycle. Moreover, the FHA can also deal with 2 DOF which are incorporated in a helical screw movement. The true flexion axis is recovered if the mentioned 2 DOF are flexion and medio-lateral tibial thrust.

For a general 6 DOF displacement the SARA or the FHA approach only approximately recover the true flexion axis. However, for the intact knee joint there exists an angular flexion range where the other 5 DOF are of minor importance such that the application of a 1 DOF model is justified. Low DOF models are convenient as they are typically numerically robust and less sensitive to data perturbations. This permits the determination of the flexion axis in a sufficiently accurate way, increasing the reproducibility of the calculated 6 DOF displacement.

4. RESULTS

Accounting for the considerations of the previous section on the validity of the FHA and SARA approaches, it is requisite to extract an angular region where flexion is the predominant motion. For this purpose, the ie-rotation as the second largest rotation is examined in the absence of noise. In the range of 0° to 45° of flexion, the original ie-rotation exhibits a large slope; at larger flexion angles, the curve flattens, and starting at about 70°, the ie-rotation increases again, see Figure 1. In order to test the performance of FHA and SARA, the axis is determined on the basis of data from a decreasing flexion interval. Subsequently, the 6 DOF displacement is represented in terms of the Joint Coordinate System (Grood and Suntay, 1983). The calculated displacement is the closer to the input displacement, the better the assumption of pure flexion is valid. Figure 1 depicts the ie-rotation which has been computed by utilizing the original flexion axis, the FHA and the SARA axis. Obviously, the results due to the original flexion axis equal the input ie-rotation.

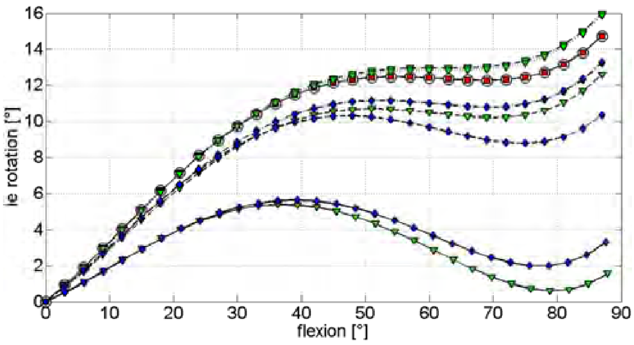

Figure 1: Internal-external (ie) rotation profile in the absence of noise. ○: ie-rotation used as input for a fictive kinematic data set.
SARA and FHA axes are determined in the flexion interval from 0° to 90° (solid lines), from 45° to 90° (dashed lines), and from 45° to 75° (dash-dotted lines).
■: Flexion-extension axis originally employed for data generation; ▼: SARA axis, ◆: FHA.

4.1 Numerical quality factor

The SARA objective function is optimized by means of a SVD, where, in the case of a planar movement (1 DOF) and absence of noise, the smallest singular value σ_6, vanishes. Influence of noise or further DOF render σ_6 finite; thus, a suitable measure for assessing the quality of the axis calculation can be based on the information contained in the singular values. We define

$$Q_{\mathrm{SARA}} = \frac{\sigma_6}{||(\sigma_1, \sigma_2, \sigma_3, \sigma_4, \sigma_5)^T||_2}. \tag{1}$$

We describe the quality of the FHA by accounting for the divergence of the set of all instantaneous helical axes (IHA) in the investigated flexion interval. As the nominal value of the quality factor is not important, this factor has been defined such that the computational cost remains moderate; in particular, multiple evaluation of trigonometric functions is avoided. We set

$$Q_{\mathrm{FHA}} = \sum_{1\le i<j\le N} \frac{2}{N\cdot(N-1)}\left(1-\left(\vec{v}_i^{\,\mathrm{iha}}\cdot\vec{v}_j^{\,\mathrm{iha}}\right)^2\right), \quad |\vec{v}_i^{\,\mathrm{iha}}| = |\vec{v}_j^{\,\mathrm{iha}}| = 1\,. \tag{2}$$

Table 1 opposes Q_{SARA} to Q_{FHA} for different flexion intervals. Both, Q_{SARA} and Q_{FHA} approach 0 for planar movement; moreover, Q_{FHA} also attains 0 for screw motion. The nominal value of Q_{SARA} cannot be directly compared to Q_{FHA}, however both factors are smallest for (45°,75°) in the unperturbed case.

interval	noise [mm]	Q_{SARA}	Q_{FHA}
$(00°, 90°)$	0	$9.2\cdot10^{-3}$	$4.7\cdot10^{-2}$
$(45°, 90°)$	0	$2.7\cdot10^{-3}$	$2.4\cdot10^{-2}$
$(45°, 75°)$	0	$4.5\cdot10^{-4}$	$2.0\cdot10^{-3}$
$(45°, 75°)$	$1-3$	$4.1\cdot10^{-4}$	$1.9\cdot10^{-3}$
$(45°, 75°)$	$5-15$	$4.7\cdot10^{-4}$	$2.2\cdot10^{-3}$
$(45°, 75°)$	$10-30$	$5.8\cdot10^{-4}$	$2.8\cdot10^{-3}$
$(45°, 70°)$	0	$4.6\cdot10^{-4}$	$2.2\cdot10^{-3}$

Table 1: Quality factors for the FHA and the SARA axis depending on the flexion range for the optimization. Q_{SARA} and Q_{FHA} are defined in eqns. (1) and (2).

The analysis of the ie-rotation profile reveals that data from the interval (45°,70°) result for both, IHA and SARA, in an ie-rotation slightly closer to the input ie-rotation than the interval (45°,75°). However, Q_{FHA} and Q_{SARA} are slightly smaller in the interval (45°,75°) than in (45°,70°). Since a larger range of motion is convenient in the presence of noise, the subsequent calculations are performed on the basis of a flexion axis, obtained – either by means of SARA or of IHA – in the flexion range of 45° to 75°.

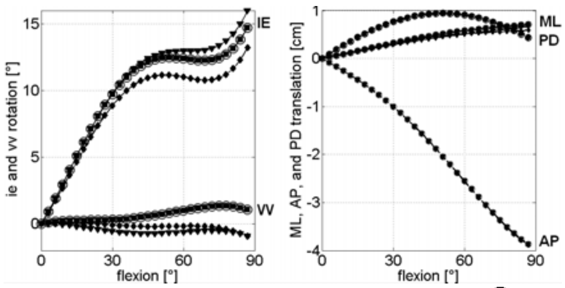

Figure 2: 6 DOF displacement in the absence of data perturbations. ○: Input 6 DOF displacement. ■:data related to the original flexion axis; ▽: data related to SARA axis, ♦: data related to FHA.

Figure 2 shows how the 6 DOF displacement is reproduced in the unperturbed case, with the FHA and SARA axes calculated in (45°,75°) of flexion. The largest relative perturbations occur for the vv-rotation and the ML-translation. Though, the absolute magnitude of these displacements is smaller compared to the remaining rotations or translations, rendering the accurate determination more difficult.

4.2 Dependence on noise

The fictive kinematic marker data are perturbed with STA (soft-tissue-artifacts)-like noise. Each marker is perturbed by a sin-function including individual amplitude, frequency, phase shift, and oscillation direction. The amplitude is selected such that the largest perturbation in consideration reaches 3 cm maximum movement of the thigh markers and 1 cm maximum movement of the shank markers. Figure 3 shows the results for the 6 DOF joint displacement in the presence of typical perturbations. Displacements involving the largest range of motion are well reproduced , i.e., flexion (which, in fact, is associated with the abscissa), ie-rotation, and AP-translation. The congruency between calculated vv-profile or ML translation and input data is poor, however, where the vv-profile cannot even be reproduced in the absence of data perturbations.

Comparing FHA and SARA axes for small perturbations, we see that SARA seems to recover the input ie-rotation data closer, whereas the other displacements are reproduced in comparable quality. For increasing noise level, the ie-rotation obtained by the FHA method is more robust than the SARA ie-rotation.

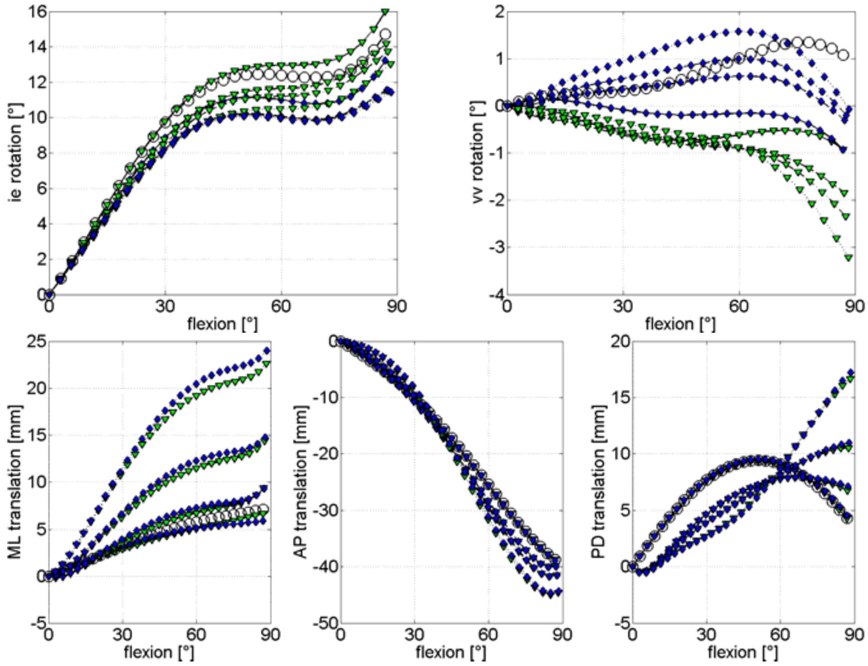

Figure 3: 6 DOF joint displacement for a maximum marker perturbation due to STA: 0 mm (solid lines), shank: 1 mm / thigh: 3 mm (dashed lines), 5 mm/15 mm (dash-dotted lines), 10 mm/30 mm (dotted lines).
○: input displacements; ▼: SARA displacements, ♦: FHA displacements.

5. DISCUSSION

A related comparison between the helical axis (HA) approach and a least squares fitting procedure has also been carried out in (Monnet et al., 2007). In contrast to the joint studied in the present contribution, they discuss a spherical joint, i.e., the shoulder. Instead of the SARA, they use the symmetrical center of rotation estimation (SCoRE) which, in fact, relies on the same objective function. These two methods may be distinguished by the rank of the least squares problem entailing two different numeric implementations (Reichl and Auzinger, 2012). Monnet et al. (2007) draw the conclusion that the HA approach is less precise than the SCoRE concerning the determination of the glenohumeral joint center. Also we found that the direction of the flexion axis is better reproduced by the SARA (Reichl and Auzinger, 2012). This may be explained by the fact that the FHA calculation yields a single reference axis for rotation and translation. In the interval (45°,75°) the largest rotational and largest translational DOF are flexion and AP-translation which are related to the flexion axis and the AP-axis. Therefore the FHA cannot equal the requested (original) flexion axis. This can only be true for data with the largest two DOF being flexion and ML-translation.

Concerning the optimization procedure, we point out that the SCoRE and the SARA approaches offer obvious advantages compared to the FHA approach. SCoRE and SARA find the axes due to a global optimization scheme whereas the IHA is only locally determined to be subsequently averaged yielding the FHA. Additionally, the FHA involves a time derivative which is highly sensitive to noise and small time increments.

In order to be able to draw practical consequences, the question if the SARA or FHA approach performs better, should be studied in the context of the type of measurement data at hand. Further investigations of the authors aim for the analysis of data obtained from alternative experimental settings such as external skin markers, medical imaging data or cadaver measurements in order to study which method is to be preferred in either case.

8. REFERENCES

1. Marin, F., Mannel, H., Claes, L., and Dürselen, L., Correction of axis misalignment in the analysis of knee rotations. Human Movement Science 2003, Vol. 22: 285–296.
2. Churchill, D. L., Incavo, S. J., Johnson, C. C., and Beynnon, B. D., The transepicondylar axis approximates the optimal flexion axis of the knee. Clin. Orthop. 1998, pages 111–118.
3. Martelli, S., Zaffagnini, S., Falcioni, B., and Motta, M., Comparison of three kinematic analyses of the knee: Determination of intrinsic features and applicability to intraoperative procedures. Computer Methods in Biomechanics and Biomedical Engineering 2002, Vol. 5: 175–185.
4. Woltring, H., de Lange, A., Kauer, J., and Huiskes, R., Instantaneous helical axis estimation via natural, cross-validated splines. In Bergmann G, Kölbel R, Rohlmann A (eds.). Biomechanics: Basic and Applied Research. Springer 1987, pages 121–128.
5. Ehrig, R. M., Taylor, W. R., Duda, G. N., and Heller, M. O., A survey of formal methods for determining functional joint axes. Journal of Biomechanics 2007, Vol. 40, 2150–2157.
6. Reichl, I. and Auzinger, W., Identifying tibio-femoral joint kinematics: individual adjustment versus numerical robustness. to appear on ifac-papersonline.net. Preprint: http://seth.asc.tuwien.ac.at/proc12/full_paper/Contribution431.pdf
7. Moglo, K. E. and Shirazi-Adl, A., Cruciate coupling and screw-home mechanism in passive knee joint during extension-flexion. Journal of Biomechanics 2005, Vol. 38, 1075–1083.
8. Dumas, R. and Chèze, L., Soft tissue artifact compensation by linear 3d interpolation and approximation methods. Journal of Biomechanics 2009, Vol. 42, 2214-2217.
9. Grood, E. S. and Suntay, W. J., A joint coordinate system for the clinical description of three-dimensional motions: Application to the knee. Journal of Biomechanical Engineering 1983, Vol. 105(2), 136–144.
10. Monnet, T., Desailly, E., Begon, M., Vallee, C., and Lacouture, P. Comparison of the score and ha methods for locating in vivo the glenohumeral joint centre. Journal of Biomechanics 2007, Vol. 40, 3487–3492.